2-4-2008

Computer Modeling and Analysis of Thermal Link Performance for an Optical Refrigerator

Kevin Byram

David Mar

John Parker

Steven Von der Porten

John Hankinson

See next page for additional authors

Authors
Kevin Byram, David Mar, John Parker, Steven Von der Porten, John Hankinson, Chris Lee, Kai Mayeda, Richard C. Haskell, Qimin Yang, Scott R. Greenfield, and Richard I. Epstein

Computer Modeling and Analysis of Thermal Link Performance for an Optical Refrigerator

Kevin Byram*[a], David Mar[a], John Parker[a], Steven Von der Porten[a], John Hankinson[a], Chris Lee[a], Kai Mayeda[a], Richard C. Haskell[a], Qimin Yang[a], Scott R. Greenfield[b], Richard I. Epstein[c]

[a]Departments of Engineering and Physics, Harvey Mudd College, Claremont, CA 91711-3116;
[b] Chemistry Division, Los Alamos National Laboratory, MS J565, Los Alamos, NM 87545;
[c] International Space & Response Division, Los Alamos National Laboratory, MS B244, Los Alamos, NM 87545

ABSTRACT

We have used the thermal modeling tool in COMSOL Multiphysics to investigate factors that affect the thermal performance of the optical refrigerator. Assuming an ideal cooling element and a non-absorptive dielectric trapping mirror, the three dominant heating factors are blackbody radiation from the surrounding environment, conductive heat transfer through mechanical supports, and the absorption of fluoresced photons transmitted through the thermal link. Laboratory experimentation coupled with computer modeling using Code V optical software have resulted in link designs capable of reducing the transmission to 0.04% of the fluoresced photons emitted toward the thermal link. The ideal thermal link will have minimal surface area, provide complete optical isolation for the load, and possess high thermal conductivity. Modeling results imply that a $1cm^3$ load can be chilled to 102 K with currently available cooling efficiencies using a 100 W pump laser on a YB:ZBLANP system, and using an ideal link that has minimal surface area and no optical transmission. We review the simulated steady-state cooling temperatures reached by the heat load for several link designs and system configurations as a comparative measure of how well particular configurations perform.

Keywords: Optical Isolation, Optical Refrigeration, Laser Cooling, COMSOL Multiphysics, Thermal Modeling

1. INTRODUCTION

The Los Alamos Solid State Optical Refrigerator (LASSOR) has demonstrated laser cooling of Yb^{3+} doped ZBLANP glass to a temperature of 208 K. The LASSOR team asked a Harvey Mudd College (HMC) clinic team to design and test optically isolating thermal links to connect thermal loads to the cooling element. The design of these thermal links should minimize absorptive reheating. The HMC team completed the project successfully, achieving optical isolation of up to 99.96% using thermal link geometries to remove light from the system. The team obtained these results by testing the link designs using a surrogate source which mimicked the optical properties of the LASSOR system. The experimental test results were confirmed by modeling the optical performance in Code V software based on non-sequential ray tracing. The team also performed thermal modeling of a LASSOR cooling element connected to a $1cm^3$ thermal load using the optical results to model absorptive reheating. The thermal modeling tool in the software package COMSOL Multiphysics was used. This paper focuses on the results of our thermal modeling which show which design would perform the best thermally.

1.1 Laser Cooling

Laser cooling uses a process called anti-Stokes fluorescence to cool materials [1]. The process of anti-Stokes fluorescence begins when a dopant ion in a glass is excited from the top energy level of the ion's ground-manifold to the bottom level of the 1st excited energy manifold. This excitation can be induced by hitting the ion with a photon of exactly the energy needed to bridge the energy gap between the two manifolds. Eventually the ion will radiatively relax to the ground-manifold, emitting a photon with at least the energy that was absorbed. In many cases the ion will transition to one of the lower energy states in the ground-manifold, and the photon emitted will carry with it more energy than the energy carried by the photon originally absorbed. The process can occur again when the ion is thermally

Laser Refrigeration of Solids, edited by Richard I. Epstein, Mansoor Sheik-Bahae,
Proc. of SPIE Vol. 6907, 69070C, (2008) · 0277-786X/08/$18 · doi: 10.1117/12.764287

excited back to the top energy level of the ground-manifold. On average the photon emitted carries more energy than the photon absorbed, so the glass cools.

The LASSOR team, in collaboration with Ball Aerospace, has used anti-Stokes fluorescence to cool Yb^{3+} doped ZBLANP by hitting the material with an infrared laser which excites it from the ground-manifold to the 1st excited manifold. In 1999 the LASSOR system demonstrated cooling to 48° below room temperature [2], and in 2005 the Ball Aerospace team demonstrated cooling of a sensor-sized load to 7° below room temperature using a thermal link [3]. The efficiency of this cooling process is small, from 1% to 3%. Because the efficiency is so low, it is important that none of the optical energy be reabsorbed by the load. Even a small amount of re-absorption would negate the cooling effects.

The cooling efficiency is also temperature dependent, so that as the temperature drops, so does the efficiency of the process [1]. Also, there is a difference between the theoretically predicted cooling efficiency and the experimentally demonstrated efficiency. In order to thermally model the system accurately, the team chose an efficiency curve based upon theory but adjusted to reflect achievable cooling rates. A full discussion appears in Section 2.2.

1.2 Designs

The design and testing of our thermal links are more thoroughly described in our companion paper [4]. However, it will be important for our discussion here to know the geometries of the different link designs as well as how each of them performed optically. We created three design alternatives that have geometries and optical interfaces which remove fluoresced photons from the system: a hemisphere design, a taper design, and a kinked waveguide design. Figure 1 shows 2-D representations of the link design alternatives. Table 1 shows the important design dimensions for each of the designs. Figure 2 is a photograph of the link prototypes we built and tested.

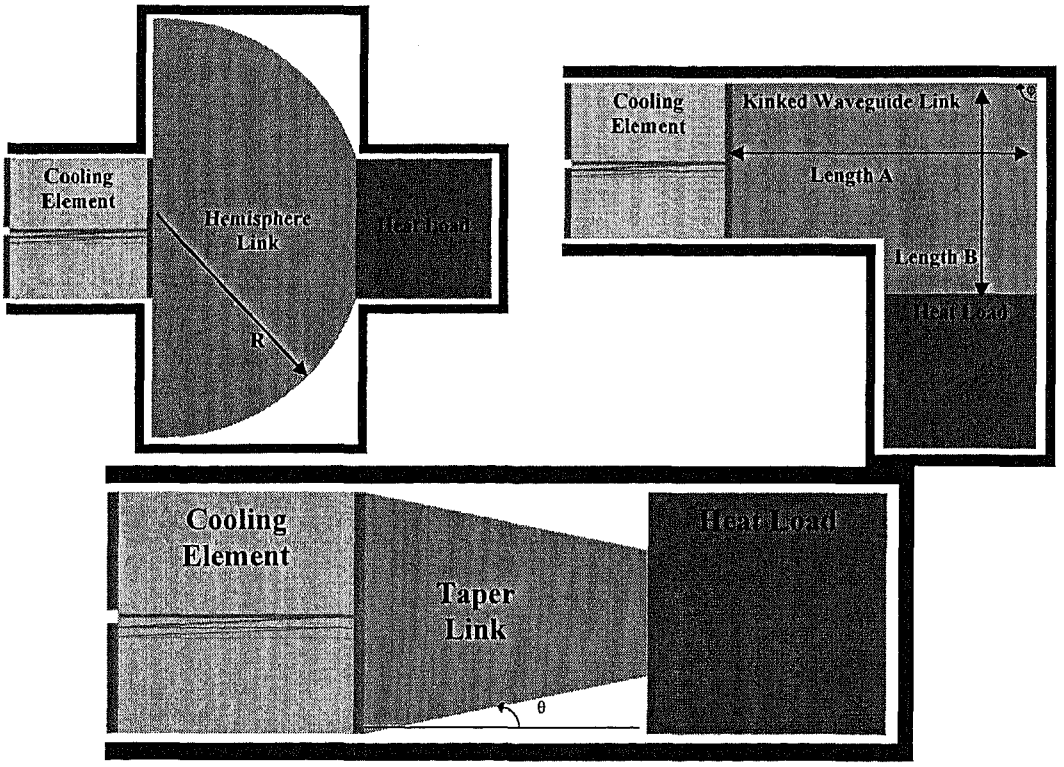

Figure 1: Link Design Geometries. The hemisphere design (top left), the kinked waveguide design (top right), and the taper waveguide design (bottom middle). The taper and kinked waveguide designs both have rectangular cross sections.

Table 1: The dimensions of the different link designs that were modeled thermally are listed below.

Design name	Dimension 1	Dimension 2	Dimension 3
Hemisphere A	Diameter - 2.9cm	End face diam. – 1.41cm	
Hemisphere B	Diameter – 3.1cm	End face diam. – 1.41cm	
Hemisphere C	Diameter – 3.8 cm	End face diam. – 1.41cm	
Hemisphere D	Diameter – 5.1cm	End face diam. – 1.41cm	
Taper A	Taper angle – 15°	Front face – 1cm x 1cm	End face–0.27cmx0.27cm
Taper B	Taper angle – 26.5°	Front face – 2cm x 2cm	End face – 1cm x 1cm
120° Kink	Cross section - 1cm x 1cm	Length A – 3cm	Length B - 4cm
90° Kink	Cross section - 1cm x 1cm	Length A – 4cm	Length B - 4cm
60° Kink	Cross section - 1cm x 1cm	Length A – 2cm	Length B – 4cm
Double 90° Kink	Cross section - 1cm x 1cm	Length A – 4cm	Length B - 4cm
Thin 120° Kink	Cross section - .25cm x .25cm	Length A – 1cm	Length B - 1cm

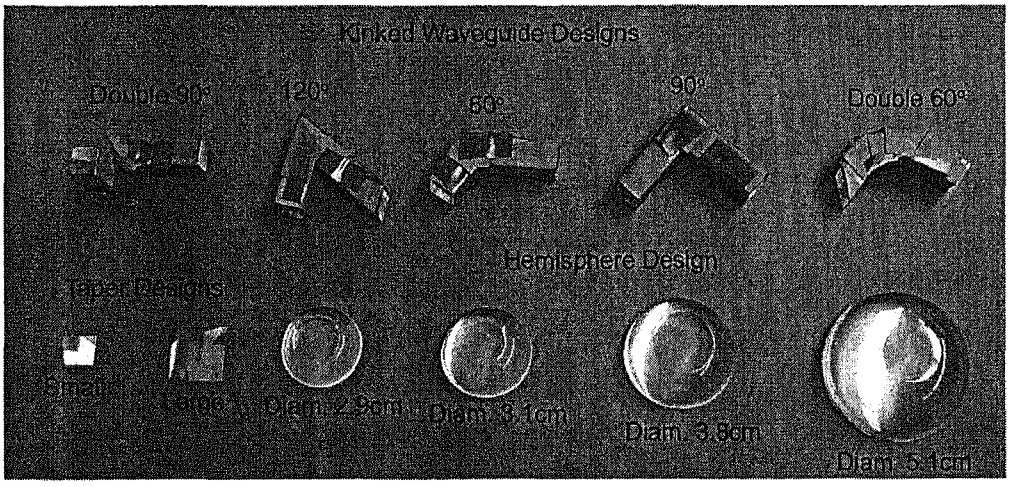

Figure 2: Link prototypes the team built and tested. The kinked waveguide designs are covered in black "baffling" which absorbs light that exits the link and prevents it from reentering the system. The double 60° kink was built and tested late in the project and is therefore not considered in the thermal modeling. The thin 120° kink is not pictured here. All of the links pictured and tested were constructed using high-optical-quality acrylic.

1.3 Surrogate Source Construction and Optical Testing

To test the optical performance of the link designs, the team constructed a surrogate source which mimicked the uniform fluorescence from the LASSOR cooling element. A dielectric mirror, similar to those used in the LASSOR system but designed for the optical wavelengths emitted by our source, was optically coupled to the output face of the surrogate

source. The optical power emitted from the output face of the surrogate source was measured using a large area ($94mm^2$) photodetector with and without the dielectric mirror. The percentage of light transmitted through the mirror/link was calculated by dividing the measured power at the exit face of the link by the power measured at the output face of the surrogate source without the mirror in place. The transmission through the dielectric mirror was 8.4%. The thermal link designs were then inserted after the mirror, with both mirror and link optically coupled, and the optical power was measured at the exit face of the link, again using the large-area photodetector. The transmission rates of the links were calculated by dividing the measured power at the exit face of the link by the power measured after the mirror, and then multiplying this number by the 8.4% transmission rate of the mirror itself. The optical transmission rates of the mirror/link designs are listed in Table 2.

Table 2: Optical transmission rates. The percentage of the total light coming through the exit face of the surrogate source transmitted through both the dielectric mirror and the thermal link.

Link Design	Optical Transmission
Hemisphere A	0.13%
Hemisphere B	0.09%
Hemisphere C	0.07%
Hemisphere D	0.06%
Taper A	0.04%
Taper B	0.60%
120° Kink	0.10%
90° Kink	1.18%
60° Kink	1.76%
Double 90° Kink	0.30%
Thin 120° Kink	.014%

The team modeled the optical performance of each of the link designs using Code V optical modeling software. The modeling results have closely matched the experimental test results. A more thorough description of the experiment as well as the optical modeling can be found in our companion paper [4].

2. THERMAL MODELING

We used COMSOL Multiphysics to model a full optical refrigeration system with a cooling element, a thermal link, a heat load, and the support fibers necessary to mechanically suspend the elements within the vacuum chamber. The software allowed us to input the geometries of the thermal link designs, the cooling element, and the heat load. The system's thermal behavior is modeled using four thermal factors that we input to the system: the cooling power of the cooling element, blackbody radiation from the surrounding environment, conductive heat transfer through the fiber supports, and absorptive heating due to photons transmitted through the thermal link and assumed to be absorbed at the heat load. The program also accepted the thermal properties of the materials and the temperature at which the system started. The program outputs both a transient temperature response as well as a final steady-state temperature distribution for the system.

2.1 Modeling the System with Designs in COMSOL

COMSOL Multiphysics allowed us to create the 3D geometries of the various subsystems. The team included the cooling element as a 1 cm^3 element of a single uniform material. The team also modeled the heat load as a 1 cm^3 element of a single uniform material, however in practice the heat load could have a more complicated shape, size, and composition. Small supports that conduct heat from the outside system were also added to both the cooling element and the heat load. The supports were cylinders 1 mm in diameter and 1 mm long of a uniform material. Finally, the team modeled the different link geometries to match the links that were modeled and tested optically. Figure 3 shows an example of a thermal model of a system utilizing the taper A link.

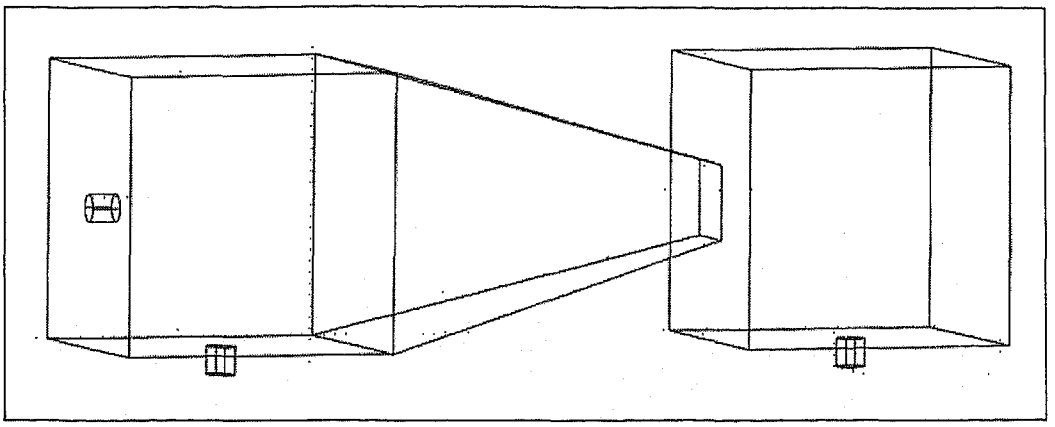

Figure 3: Example structure of a system for thermal modeling. This figure shows the underlying physical structure for an example model constructed in COMSOL. The cubic cooling element is at left, the cubic heat load is at right, and the thermal link (taper A, in this case) is in the middle. There is a small cylindrical support fiber at the bottom of both the cooling element and the heat load. In addition, the model included a small cylinder in the cooling element of different material to model the hole in the trapping mirror where the pump laser enters the system.

2.2 COMSOL Input Parameters

The software also allowed us to set parameters for both the thermal and material properties of the systems. There are two types of properties the team can set: subdomain settings which act over volumes, and boundary surface conditions.

We first modeled the material properties of the system as subdomain settings. The thermal properties of a material include the material's density, specific heat, and thermal conductivity. The thermal properties of ZBLANP were used to model the cooling element. The thermal properties of ZBLANP were also used for the support fibers because the LASSOR system's support fibers are currently made of ZBLANP. In reality, the support fibers on the heat load will be a different material, however it is unknown what that material will be. The thermal properties of copper were used to model the heat load because of copper's high thermal conductivity. As a result, the heat load maintained a relatively constant temperature throughout its volume when compared to the rest of the system. Initially, the thermal properties of silica glass were used to model the thermal links, but any link material can be used. The effect of changing the thermal properties on the steady-state temperature is discussed in Section 3.3.

The cooling power, heat load, and heating due to optical absorption were also modeled as subdomain settings. The cooling properties of the cooling element were included in the model by applying a volumetric cooling term to the cubic cooling element. The software calculated the magnitude of the cooling term using the input pump laser power, the volume of the cooling element, and a temperature dependent cooling efficiency. The pump laser power was initially assumed to be 5 W. The effects of changing this laser power are discussed in Section 3.3. The cooling efficiency's temperature dependence followed a curve fit shown in Figure 4. The figure shows the theoretically predicted cooling efficiency and the actual cooling efficiency achieved by LASSOR. We decided to use the ideal efficiency which had a well-defined equation, but following the suggestion of the LASSOR team, we scaled the efficiency down by a factor of 3 to more closely reflect the measured cooling efficiency.

Similar to the procedure used for the cooling element, the team could have included a volumetric heat source generated in the heat load region. The thermal nature of the heat load is expected to vary by application, so we chose not to generate any heat in the load. We did, however, include a heat source in the load due to the optical leakage of the link designs. To do this, we first determined the thermal links' transmission rates as described in Section 1.3. We then determined the power of the optical heat load by multiplying the optical transmission of the mirror/link system by 1/6 of the pump laser power. The factor of 1/6 was used because it was assumed that the fluorescent light was emitted isotropically and therefore only 1/6 of the pump laser power would exit the face of the cube to which the mirror and link were attached. The amount of optical power converted to heating was included in our models as volumetric heat

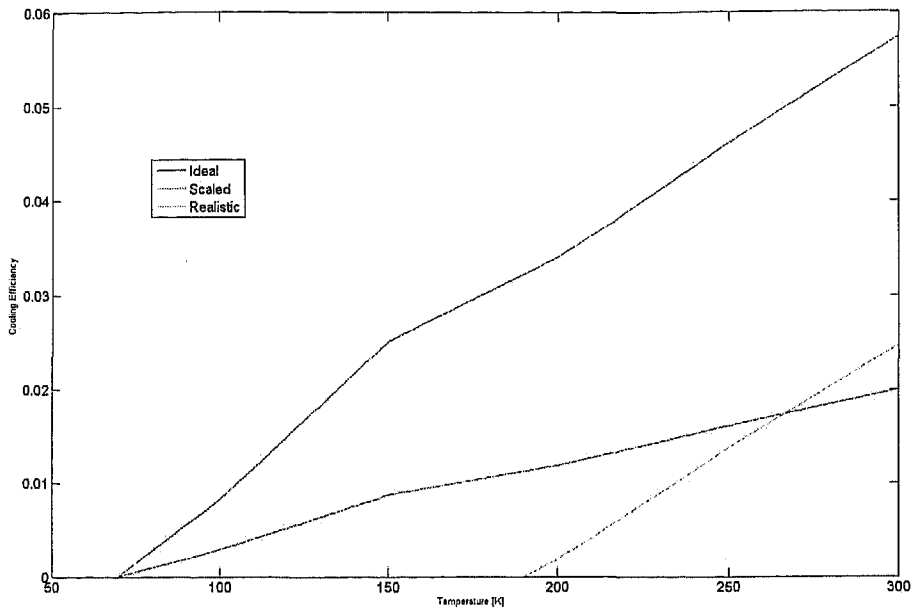

Figure 4: Cooling efficiency as a function of temperature within the cooling element. This figure shows the ideal cooling efficiency attainable by the ZBLANP system as a function of temperature in blue. The data was supplied by the LASSOR team. The red line corresponds to scaled values of the ideal efficiency used by the team. The values were scaled such that the efficiency at 300 K is 0.02. This value was suggested as a more realistic efficiency range.

generation across the entire volume of the heat load.

In addition to the material properties and volumetric heat terms, we modeled as boundary conditions at the surface of the system the heat that would be absorbed due to thermal radiation from the chamber walls, as well as the heat that would conduct into the system through the support fibers. To model the radiative heat term, we set the chamber walls to a constant 300 K, and set the emissivity of the walls to be 0.1. Setting the emissivity to 0.1 meant that 10% of the energy that a perfect blackbody would radiate would be radiated by the walls. It also meant that the walls would absorb only 10% of the radiation from the system, and the other 90% of the radiation would be reflected back toward the system. The low emissivity of the chamber walls can be achieved by coating the chamber walls with a coating that has a low emissivity. We also included the effects of a small, high-emissivity window through which the pump laser enters the system, since this hole cannot be coated with a low emissivity (high reflectivity) material. This window is shown as a 1 mm diameter cylinder in Figure 3 on the left end of the cooling element. The effects of lowering the emissivity below 0.1 are examined in Section 3.3. We assumed that the walls were positioned very close to the surfaces of the system so that the total absorptive surface area of the system is equal to the total radiative surface of the chamber. Holding the walls close will be necessary for the modeling to calculate the radiative heat load, and it will be necessary in the actual system to make sure that light escaping the system does not later reenter the system.

Since the LASSOR system is assumed to be held in vacuum, the only heat conduction between the system and the chamber was through the support fibers. To model this, the ends of the support fibers at the chamber walls were held at 300 K. Additionally, the entire system was assumed to start at a uniform temperature of 300 K.

2.3 Thermal Analysis

The software calculates the thermal inputs across the system at a given time and then determines the changes in temperature throughout the system. The program applies these changes and then recalculates the thermal inputs for the next step forward in time. The software steps through iterations of this process until a steady state convergence criterion

is reached. Once the model has been completed, the software can output both the transient temperature response and the steady-state temperature distribution and heat flow in three ways. First, the program can evaluate and output the temperature at a given point in the system. Second, it can evaluate the heat flux through a specified surface. Finally, the program can evaluate the average temperature over a specified volume. The software outputs results numerically and with graphic visualizations. An example of the graphical output is shown in Figure 5.

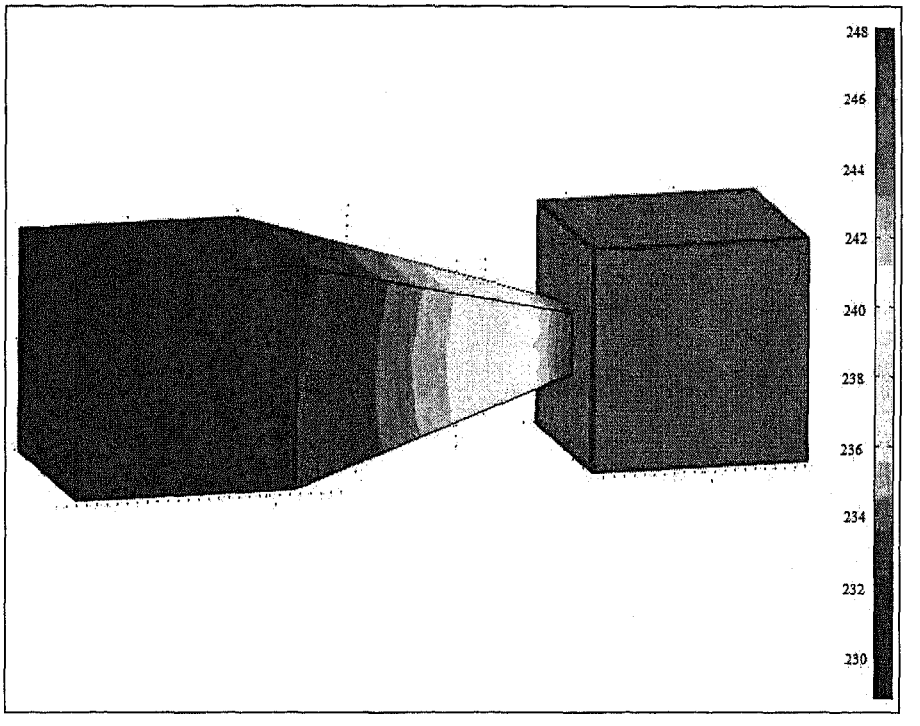

Figure 5: Temperature gradient over Taper A. This figure shows the visualization output from the thermal modeling software. The temperature scale goes from 230 K (blue) to 248 K (red).

3. RESULTS

This section describes the results obtained from thermally modeling the refrigeration system using different thermal link designs. A summary is presented of the relative magnitude of the different heating factors: the cooling power of the cooling element, the radiative power absorbed from the chamber, the power conducted into the system through the support fibers, and the optical power absorbed at the load.

3.1 Thermal Heating Factors

The four power factors that contribute to the final temperature of the system and their steady state magnitudes are listed in for systems using each of the link designs. The "no link/load" case was performed with just a cooling element to determine the minimum possible temperature a stand-alone cooling element could reach. The "zero optical leakage" case was performed by placing a heat load directly next to a cooling element but eliminating all optical transmission. The "no link" case was modeled similarly, but the optical transmission was set to 8.4%, the transmission rate of the trapping dielectric mirror.

Table 3: Magnitude of thermal factors using a 5 W pump laser. Designs are sorted by the temperature reached at the heat load of the system, with the coolest designs listed first.

	Cooling Power [mW]	Surface Area Radiative Load [mW]	Fluorescence Absorb Power [mW]	Conductive Power [mW]
No Link/Load	-61.5	22	0	39.7
Zero Optical Leakage	-77	29	0	52.6
Taper A [1]	-79.5	35	0.3	47
Thin 120° Kink [1]	-81.1	28.5	0.1	41.7
Taper A	-77	34	0.3	45
Taper B	-82	40.1	5	39
Hemisphere A	-83.9	45.7	1.1	35.7
Hemisphere B	-85	50	0.8	33
120° Kink [1]	-86	62	1	31
Double 90° Kink [1]	-86	71	2.5	21
60° Kink [1]	-87.2	57.5	15	28.3
Hemisphere C	-87	56	0.6	28
90° Kink [1]	-88	57	9.9	28
Hemisphere D	-90	66	0.4	20
No Link	-93	9	71	13.6

[1] A thermal conductivity of 41 W/(m·K) (approx. sapphire) was used for these links (1.38 W/(m·K) for others). See Section 0 for more details.

The first heat source listed is the cooling power provided by the cooling element. The cooling power is determined using the power of the pump laser, the temperature of the cooling element, and the efficiency of the cooling element at that temperature. The higher the pump laser power, the higher the cooling power. The lower the temperature of the cooling element, the lower the cooling power.

The second source listed is the heating due to thermal radiation from the chamber walls. This heat load is calculated using the emissivity of the walls, the exposed surface area of the entire system (cooling element, link, and load), and the temperature difference between the walls (held at 300 K) and every surface point on the system. This factor was larger in link designs with larger surface areas. This factor was also larger in designs that reached colder temperatures and therefore had larger temperature differences, however the exposed surface area had a much larger impact on the radiative load than did the temperature difference. The surface areas of the links as well as their optical transmission are shown in Table 4.

The third heat source is the heat generated in the system through optical absorption which was calculated as described in Section 2.2 using the power of the pump laser used to cool the system and the optical transmission rate of each specific mirror/link system. This power is constant over time for each specific mirror/link system. We used the transmission rates of the different mirror/link systems obtained experimentally as shown in Table 4. Note that in the "no link/load" and "zero optical leakage" cases the optical absorption is set to 0, and in the "no link" case it is set to 8.4%, the measured optical power leaked by the dielectric mirror.

The final heat source is the power that conducts into the system through the support fibers. This factor is determined by the conductivity of the support fibers and the temperature difference between the two ends of the support fiber. Links that achieve lower temperatures have larger conductive loads. The difference in the conductive heat loads in the different links is due entirely to the differences in temperature achieved by the different links.

Table 4: Key link characteristics. The total surface area for the link designs and the optical transmission rates of the mirror/link system that were determined experimentally are shown.

Link Type	Surface Area (cm^2)	Optical Transmission
No Link/Load	6.07	0%
Zero Optical Leakage	10.07	0%
No Link	10.07	8.4%
Hemisphere A	26.71	0.13%
Hemisphere B	30.9	0.09%
Hemisphere C	41.49	0.07%
Hemisphere D	68.17	0.06%
Taper A	14.57	0.04%
Taper B	19.78	0.60%
90° Kink	35.99	1.18%
60° Kink	29.96	1.76%
120° Kink	35.56	0.10%
Double 90° Kink	40.7	0.30%
Thin 120° Kink	19.4	.014%

Figure 6 shows the relative magnitudes of the different heat terms graphically. The cooling element power is not shown because it is approximately the sum of the other three factors. The cooling power is not exactly the sum of the other terms because the steady state convergence criterion led to a round-off error of up to 10%. Obviously in the "no link" case the absorptive load dominates the system. In all other systems, the absorptive load is small compared to the radiative and conductive loads. In the systems that achieved lower temperatures at the heat load, such as taper A and the thin 120° kink, the absorptive load is negligible, and the conductive and radiative loads are approximately equal. In systems that performed worse thermally, even though there was good optical performance, the thermal behavior is dominated by much larger radiative loads due to large surface areas. The large radiative load is what prevented these systems from reaching lower temperatures.

3.2 Achievable Load Temperatures

The steady state temperatures achieved by the different links in the case of a 5 W pump laser are shown in Table 5. The table lists the temperature reached at a point at the middle of the heat load, as well as the temperature reached at a point at the middle of the cooling element. The table also includes the temperature difference between the heat load and the cooling element. This temperature difference is important because if a link cannot effectively conduct heat from the heat load to the cooling element, it will not be thermally effective. Several of the designs, particularly the kinked waveguide designs, had very large temperature differences because they had longer distances across which the heat must flow. In these designs the temperature differences were so large that these link designs were ruled out as feasible solutions. For example, the 90° kinked waveguide had a temperature difference of 40 K.

One way to lower the temperature difference between the heat load and the cooling element is to make the thermal links out of a material with a higher conductivity. Glass has a thermal conductivity of 1.38 W/(m·K). An alternative material suggested by LASSOR is sapphire, which has a thermal conductivity of 41 W/(m·K). However, sapphire has an index of refraction of 1.8 instead of 1.5, which would change the optical properties and performance of the links.

While most links were modeled with the thermal properties of glass, we decided to model the kinked waveguide designs using the thermal conductivity of sapphire to lower the temperature difference between the heat and the load and make the kinked waveguide designs competitive with the other designs. However, since the physical links were constructed of acrylic, no data was available on how the links would perform optically with an index of refraction of 1.8. Therefore the team used the optical transmission rate determined experimentally with an index of refraction of 1.5 (acrylic PMMA), and changed only the thermal conductivity of the material in the thermal model. The team modeled the taper A design with the thermal properties of both silica glass and sapphire because it reached the lowest temperature at the heat load using the thermal properties of silica glass.

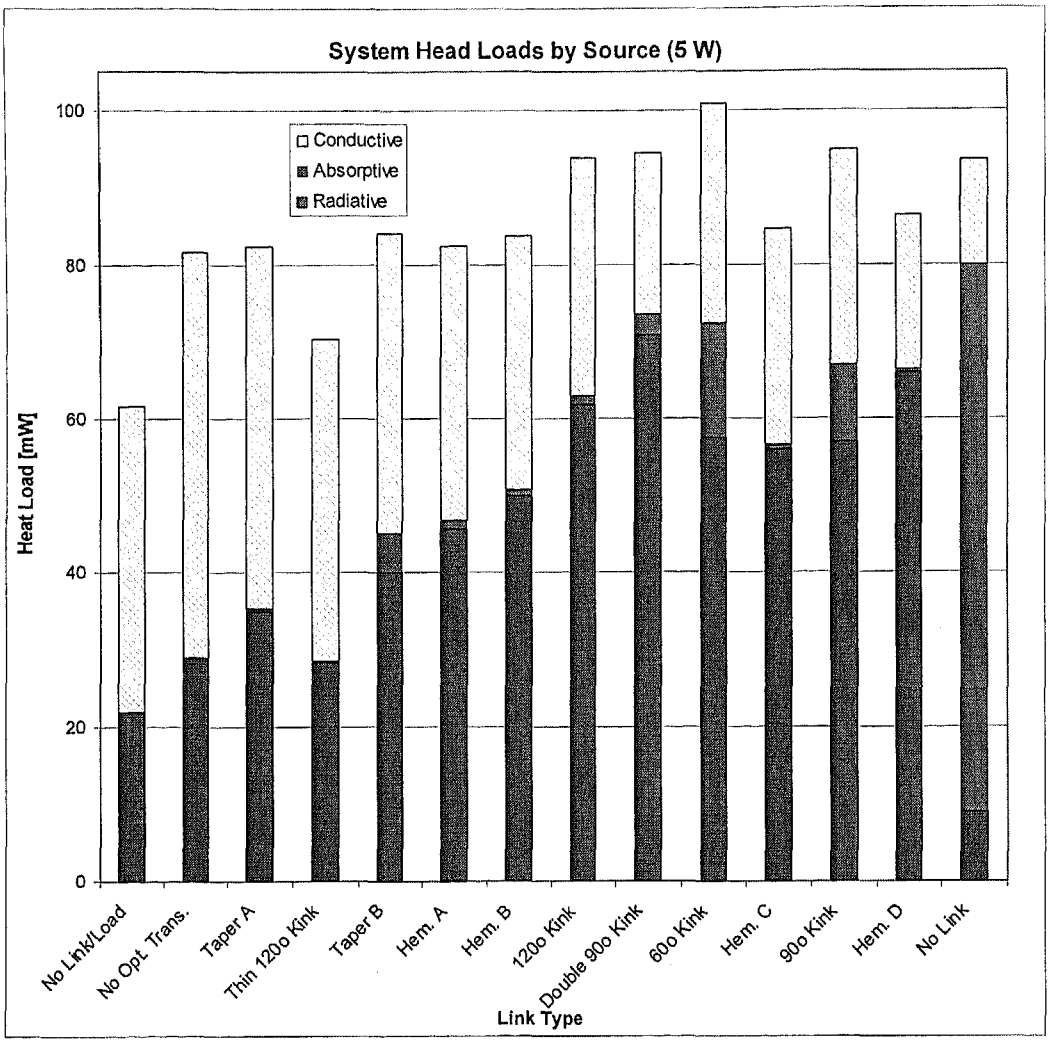

Figure 6: System heat loads for various link designs. This figure shows the relative contribution of the three heating effects in the systems for a 5 W pumping laser power. Links are ordered in the x-direction from coolest final temperature on the left to warmest on the right.

Based on the final achievable temperature, the small taper design, taper A, performed the best thermally. The thin 120° kink performed the best optically, however it did not perform the best thermally. The reason for this is that the cross-sectional area of the link was small, the distance through which heat must flow was large, and therefore the link was unable to effectively conduct heat from the heat load, down the link, and to the cooling element. Taper A, on the other hand, had a comparatively large cross-sectional area and a small distance between the cooling element and the load. It was able to conduct thermal energy efficiently down the link.

One way to reduce the radiative load is to lower the emissivity of the chamber walls. Lowering the emissivity will allow the links to reach a cooler temperature by decreasing the magnitude of the radiative load. As an example, reducing the emissivity of the walls from 0.1 to 0.02 reduced the temperature that the Taper A design reached from 249 K to 238.5 K, and the radiative load fell from 35 mW to 15 mW.

Table 5: System Temperature Results. The final steady state temperatures found using a 5 W pump laser power. Links are sorted by the temperature reached at the load.

	5 W Load Temp [K]	5 W CE Temp [K]	5 W Temp. Difference [K]
No Link/Load	205	205	0
Zero Optical Leakage	249	246.6	2.4
Taper A [2]	255	252	3
Thin 120° Kink [2]	261	255	6
Taper A	262	256	6
Taper B	263	258	5
Hemisphere A	267	261	6
Hemisphere B	269	264	5
120° Kink [2]	271	267	4
Double 90° Kink [2]	271	267	4
60° Kink [2]	273	269	4
Hemisphere C	274	268	6
90° Kink [2]	274	270	4
Hemisphere D	282	276	6
No Link	288	283	5

[2] A thermal conductivity of 41 W/(m·K) (sapphire) was used for these links while 1.38 W/(m·K) was used for the others. See Section 0 for more details.

3.3 Effects of Input Parameters

As seen in the previous section, different material conductivities lead to changes in the final temperatures achieved by the heat loads. Specifically, increasing the conductivity of the links lowered the final achievable temperatures. In addition, input parameters such as the input laser power also affects the overall system performance. This section focuses on additional tests regarding the effect of changing various input parameters on the system.

We first performed a test in which the pump laser power input was increased from 5 W to 100 W. It was assumed that even with greater pump laser power the efficiency characteristics of the cooling element would remain the same. Changing the laser power increases the cooling power of the cooling element but also increases the optical absorption due to more fluorescence photons finding their way down the link. The steady state temperatures and power magnitudes in the high input laser power case are listed in Table 6. The relative power magnitudes are graphed in Figure 7.

We found that by increasing the laser power, the final temperature the heat load can reach is substantially lower. Also, the relative magnitude of the absorptive load is increased substantially. In the "no link" system, this actually caused a net heating effect, and the total optical absorption power is off the chart. In links such as the Taper A design that performed well optically, even with a 100 W laser pumping power the optical absorption is still negligible compared to the other two heating effects. This implies that our links perform very well optically, and that it is more important now to find ways to minimize the conductive heat load and the radiative heat load.

Table 6: System temperature and heat power results: high-power (100 W) case.

	Cooling Power [mW]	SA Rad. Load [mW]	Absorb Power [mW]	Cond. Power [mW]	100 W Load Temp [K]	100 W CE Temp [K]	Temp. Difference [K]
No Link/Load	-119	28.4	0	91.4	83	83	0
No Optical Transmission	-250.7	62.6	0	204	102	94.8	7.2
Taper A [3]	-274	83	6.9	201.2	107.2	96.7	10.5
Thin 120° Kink [3]	-284	55	2.1	194.6	117	98	19
Hemisphere A	-332	117	21	191	120	101	19
120° Kink [3]	-370	210	19.7	193	120	104	16
Double 90° Kink [3]	-360	231	51	127	122	103	19
Hemisphere B	-344	140	15	189	123	102	21
Hemisphere C	-381	182	12	184	129	105	24
Taper B	-372	99	100	184	130	104	26
Hemisphere D	-460	296	8.3	154	143	111	32
90° Kink [3]	-526	201	197	172	145	117	28
Taper A	-248	75	6.9	177	149	94	32
60° Kink [3]	-590	212	298	161	154	122	32
No Link	-1467	12.5	1427	27	306	224	82

[3] A thermal conductivity of 41 W/(m·K) (sapphire) was used for these links (1.38 W/(m·K) for others). See Section 0 for more details

4. CONCLUSIONS

We have developed optically isolating thermal links to thermally couple an optical refrigerator to a heat load. It is clear from the thermal modeling performed on these links that the optical isolation is sufficiently high that heating from optical absorption is negligible compared to other thermal factors. Therefore, in order to further improve the cooling capabilities of optical refrigerators, the team recommends that efforts be focused on reducing the other thermal factors. These include reducing the heat that flows into the system through the support fibers, and the thermal radiation absorbed by the system from the chamber walls. To reduce conduction into the system, support fibers can be made with more insulating material. To reduce the radiative load, the emissivity of the chamber can be lowered, or link designs which minimize exterior surface area can be chosen. One way to reduce both of these factors is to reduce the temperature of the chamber walls, possibly using a multistage cooling system. We did not pursue this possible design pathway because a multistage cooling system is likely to lose the benefits of laser cooling such as the absence of vibrations.

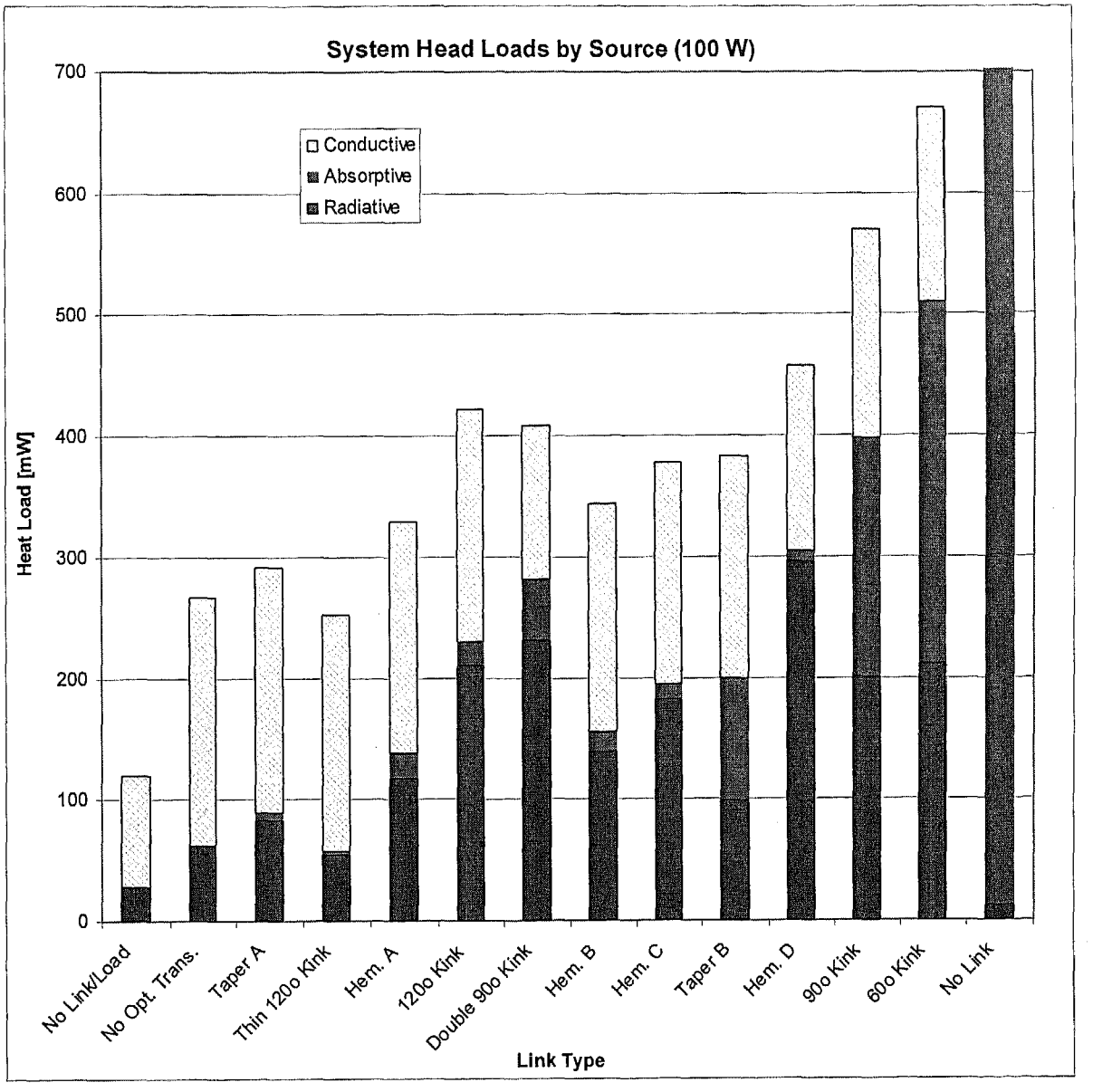

Figure 7: System heat loads using a 100 W laser pump power. Links are ordered from left to right with the coolest final temperature on the left and the warmest on the right.

5. ACKNOWLEDGMENTS

This work was performed under a Harvey Mudd College joint Physics-Engineering clinic project funded by Los Alamos National Laboratories. The authors would like to thank the Los Alamos Solid State Optical Refrigerator team for their help and insights during this project. The authors would also like to thank the Harvey Mudd Clinic Program for providing the structure and support needed to undertake the project.

REFERENCES

[1] R. Epstein, J. Brown. B. Edwards. A Gibbs. "Measurements of Optical Refrigeration in Ytterbium-doped Crystal." J. Appl. Phys. **90(9)**, 4815-4819 (2001).

[2] B. Edwards, J. Anderson, R. Epstein, G. Mills, A. Mord. "Demonstration of a solid-state optical cooler: an approach to cryogenic refrigeration." J. Appl. Phys. **86(11)**, 6489-6493 (1999).

[3] G. Mills and A. Mord. "Modeling the performance of an optical refrigerator." NASA ESTO Conf. 2005.

[4] J. Parker, D. Mar, J. Hankinson et al. "Designs and Optical Tests of Thermal Links for an Optical Refrigerator." Photonics West Conf. 2007.

[5] G. Mills, J Fleming, Z. Wei, J Turner-Valle. "Optical Cryocooling and the Effects of Dielectric Mirror Leakage." NASA ESTO Conf. 2002.

[6] Phillips Lumileds Lighting Company. *Technical Data Sheet DS46.* <http://www.lumileds.com/pdfs/DS46.pdf>